Drug Development and Industrial Pharmacy, 2009; 35(9): 1128–1138

informa
healthcare

ORIGINAL RESEARCH PAPER

Dissolution rate enhancement of the poorly water-soluble drug Tibolone using PVP, SiO_2, and their nanocomposites as appropriate drug carriers

Sofia Papadimitriou and Dimitrios Bikiaris

Laboratory of Organic Chemical Technology, Department of Chemistry, Aristotle University of Thessaloniki, Thessaloniki, Greece

Abstract

Background: Creation of immediate release formulations for the poorly water-soluble drug Tibolone through the use of solid dispersions (SDs). *Aim*: SD systems of Tibolone (Tibo) with poly(vinylpyrrolidone) (PVP), fumed SiO_2 nanoparticles, and their corresponding ternary systems (PVP/SiO_2/Tibo) were prepared and studied in order to produce formulations with enhanced drug dissolution rates. *Method*: The prepared SDs were characterized by the use of differential scanning calorimetry and wide-angle X-ray diffractometry techniques. Also dissolution experiments were performed. *Results*: From the results it was concluded that PVP as well as SiO_2 can be used as appropriate carriers for the amorphization of Tibo, even when the drug is used at high concentrations (20–30%, w/w). This is due to the evolved interactions taking place between the drug and the used carriers, as was verified by Fourier transform infrared spectroscopy. At higher concentrations the drug was recrystallized. Similar are the observations on the ternary PVP/SiO_2/Tibo SDs. The dissolution profiles of the drug in PVP/Tibo and SiO_2/Tibo SDs are directly dependent on the physical state of the drug. Immediately release rates are observed in SD with low drug concentrations, in which Tibo was in amorphous state. However, these release profiles are drastically changed in the ternary PVP/SiO_2/Tibo SDs. An immediate release profile is observed for low drug concentrations and an almost sustained release as the concentration of Tibo increases. This is due to the weak interactions that take place between PVP and SiO_2, which result in alterations of the characteristics of the carrier (PVP/SiO_2 nanocomposites). *Conclusions*: Immediate release formulation was created for Tibolone as well as new nanocomposite matrices of PVP/SiO_2, which drastically change the release profile of the drug to a sustained delivery.

Key words: *Dissolution rate enhancement; PVP; silica nanoparticles; solid dispersion; Tibolone*

Introduction

Solid dispersion (SD) seems to be one of the most successfully used method for the improvement of the dissolution properties of poorly water-soluble drugs minimizing the limitations of oral bioavailability[1–5]. According to the Noyes–Whitney equation, the most attractive and easy way to enhance the release rate of the drug is to increase its surface area by reducing the particle size rather than to increase drug solubility[6–8]. Additionally, factors that can contribute to this direction are to optimize the wetting characteristics of the compound surface, decreasing the boundary layer thickness, ensuring appropriate conditions for dissolution and improving the apparent solubility of the drug under physiologically relevant conditions[9]. Water-soluble polymers are widely and repeatedly used as carriers of solid dispersions, from which drugs are released quickly[10].

Poly(vinylpyrrolidone) (PVP) is a readily water-soluble macromolecular compound, as well as in most common polar organic solvents, such as alcohols, amines, acids, and chlorinated hydrocarbons, exhibiting exceptional low toxicity and high biocompatibility. It is found in the form of a white powder, with many applications

Address for correspondence: Professor Dimitrios Bikiaris, Laboratory of Organic Chemical Technology, Department of Chemistry, Aristotle University of Thessaloniki, 541 24 Thessaloniki, Greece. Tel: +30 2310 997812, fax: +30 2310 997769. E-mail: dbic@chem.auth.gr

(Received 2 Jun 2008; accepted 30 Jan 2009)

ISSN 0363-9045 print/ISSN 1520-5762 online © Informa UK, Ltd.
DOI: 10.1080/03639040902787653

as drug carrier in pharmaceutical technology[11]. It is highly hygroscopic, absorbing about 30% of water at 60% humidity. An alternative drug carrier that has been used for the improvement of the dissolution rate of poorly water-soluble drugs is SiO_2 nanoparticles[12,13]. Amorphous silicon dioxide was first produced 60 years ago and since then has become a truly multifunctional filler with a variety of applications in different industries. It is used as a filler, performance additive, rheological modifier, or processing aid in many product formulations in pharmaceutical technology. Silicas having many silanol groups on their surfaces are capable of forming hydrogen bonds with drug molecules. Thus the drug is molecularly dispersed on the silica's surface[14]. These two excipients have been also used together in ternary SD systems with two different drugs, Carvedilol and Simvastatin, showing a significant improvement of the drug release profile in both cases[15,16]. In this study, these carriers as well as their PVP/SiO_2 nanocomposites were used comparatively for the dissolution rate enhancement of Tibolone (Tibo), which is a poorly water-soluble drug.

Tibo [(7a,17a)-17-hydroxy-19-nor-17-pregn-5(10)-en-20-yn-3-one] is a synthetic steroid known to have combined estrogenic, progestogenic, and androgenic characteristics. It is structurally related to the progestogens, norethindrone and norethynodrel, and it is a known tissue-specific and effective agent that can be used in hormone replacement therapy (HRT) in (post)menopausal woman, for the treatment of menopausal and postmenopausal disorders, including climacteric complaints, vasomotor symptoms, osteoporosis, and vaginal atrophy[17–23]. The already published papers concerning the dissolution rate enhancement of Tibo are limited[24].

In this study, SDs of Tibo with PVP, SiO_2, and PVP/SiO_2 nanocomposites were prepared using the solvent evaporation technique, in order to increase the dissolution rate of Tibo. In ternary SDs different proportions of SiO_2 and drug were used. These systems were characterized in comparison with pure Tibo drug in order to identify the role of the carriers and different drug proportions on the release profile of the drug.

Experimental

Materials

Crystalline Tibo with an assay 99.59% was supplied from Zhejiang Xianju Junye Pharmaceutical Co. Ltd. (Hebu Bridge, Xianju, Zhejiang, China) PVP type Kollidon K30 with a molecular weight M_w of 50,000–55,000 was obtained from BASF (Ludwigshafen, Germany), T_g = 167°C (DSC), moisture content 1.95% (TGA), and bulk density 0.410 g/cm^3. Hydrophilic fumed silica (SiO_2) nanoparticles having a specific surface area 200 m^2/g and SiO_2 content >99.8% were supplied by Degussa AG (Hanau, Germany) under the trade name AEROSIL® 200. Ethanol absolute was obtained from Merck (Darmstadt, Germany). All the other materials and reagents were of analytical grade and purity.

Preparation of solid dispersions

SDs of fumed silica nanoparticles (SiO_2) containing 10%, 30%, and 50% (w/w) Tibo were prepared by dissolving the drug in ethanol and adsorbing these solutions onto the surface of silica with the use of gentle mixing. Corresponding samples of PVP/Tibo were also prepared containing 10%, 30%, and 50% (w/w) Tibo by dissolving the drug and polymer to ethanol under gentle mixing. Another series of samples were prepared using mixtures of PVP/SiO_2 nanocomposites with constant weight ratio 85/15% (w/w) containing 10%, 20%, 30%, 40%, and 50% (w/w) Tibo. These samples were also prepared with the solvent evaporation method. The final solutions were poured onto aluminum plates. Solvent was left to evaporate at room temperature. After complete removal of the solvent in all the samples, the powder of the SDs was stored at 25°C in a desiccator.

Differential scanning calorimetry

Thermal analysis of the samples was carried out using a PerkinElmer Pyris-1 DSC (Waltham, MA, USA). The calorimeter was calibrated with Indium and Zink standards. For each measurement a sample of approximately 6 mg was used, placed in aluminum seal, and heated at 130°C at a heating rate of 20°C/min. The sample remained at that temperature for 10 minutes in order to erase any thermal history and remove the moisture traces. The samples were quenched at 0°C and scanned again up to 200°C using the same heating rate.

Wide-angle X-ray diffractometry

Wide-angle X-ray diffractometry (WAXD) was used for the identification of the crystal (structure and changes) properties of the pure materials and dispersion systems. WAXD study was performed over the range 2θ from 5° to 50°, using a Philips PW 1710 diffractometer with Bragg-Brentano geometry (θ, 2θ) and Ni-filtered CuKa radiation.

Fourier transform infrared spectroscopy

Fourier transform infrared spectroscopy (FTIR) spectra were obtained using a PerkinElmer FTIR spectrometer, model Spectrum 1000. In order to collect the spectra, a small amount of each material was used (1 wt%) and compressed in KBr tablets. The IR spectra, in absorbance

mode, were obtained in the spectral region of 450–4000 cm^{-1} using a resolution of 2 cm^{-1} and 64 co-added scans.

Dynamic mechanical analysis

The dynamic thermomechanical properties of the PVP/SiO_2 nanocomposites were measured with a PerkinElmer Dynamic Mechanical Analyzer (model Diamond). The bending method was used at a frequency of 1 Hz in the temperature ranging from 30°C to 200°C. The heating rate was 3°C/min. Testing was performed using rectangular bars measuring approximately $30 \times 10 \times 0.5$ mm^3. The exact dimensions of each sample were measured before the scan.

Scanning electron microscopy

The morphology of the prepared SDs was examined by a scanning electron microscopy system (SEM) Jeol. The samples were covered with carbon black in order to increase conductivity of the electron beam. Operating conditions were accelerating voltage 20 kV, probe current 45 nA, and counting time 60 seconds.

Release profile

In vitro drug release studies were performed as follows. Dissolution apparatus I basket method was used. SD samples corresponding to 2.5 mg Tibo were placed in soft gelatin capsules, and placed into the baskets. Dissolution medium consisted of 500 mL water and 0.25% sodium lauryl sulfate (pH 7), the stirring rate was kept constant at 100 rpm, and the temperature also at 37°C[23]. At predetermined time intervals 3 mL of aqueous solution was withdrawn from the release media. The samples were filtered and the quantitation analysis was performed by using a Shimadzu HPLC (model LC-20AD). The column used was a Hypersil BDS, 5 μm, 200×4.6 mm^2 with a column temperature at 30°C. The mobile phase consisted of methanol/water 77/23 (v/v) at a flow rate of 0.8 mL/min. Concentration determination was performed using UV detection at a wavelength 205 nm. Previously, an appropriate calibration curve was created.

Results and discussion

Characterization of solid dispersions

Differential scanning calorimetry

In order to evaluate how the methods used to prepare SDs have affected the physical properties of the drug, DSC was used. Tibo is a crystalline compound with a melting point of 169–173°C, maximum at 171°C. After quenching it can be made completely amorphous, with a glass transition temperature (T_g) at 52°C (Figure 1). During heating above the T_g it crystallizes at a cold crystallization temperature of (T_{cc}) 87.5°C, while its melting point remains identical with the previously reported for pure Tibo. Additionally, the shape of the melting peak remains the same, without the existence of other peaks, indicating that thermal treatment does not affect the form, as well as the purity of Tibo. When the drug is cooled with a slow cooling rate from its melting point it crystallizes rapidly (T_c) at 134°C.

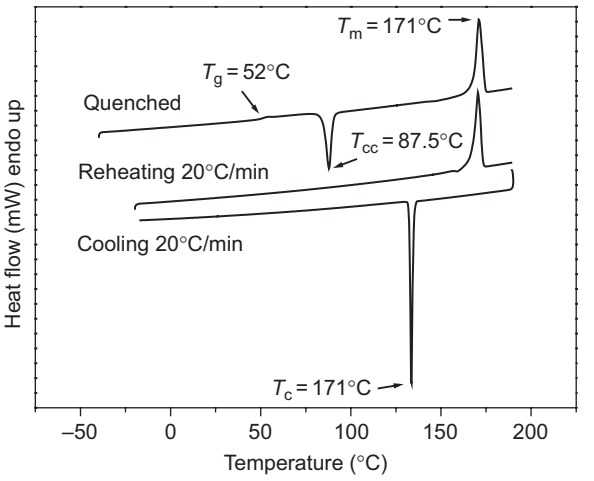

Figure 1. DSC thermograms of pure Tibo.

The thermograms for two different series of binary SDs were recorded and presented in Figures 2 and 3. In the case of SiO_2/Tibo SDs, DSC thermograms show that the drug seems to be amorphous for the sample of SiO_2/Tibo 90/10% (w/w), as no melting point is recorded. For

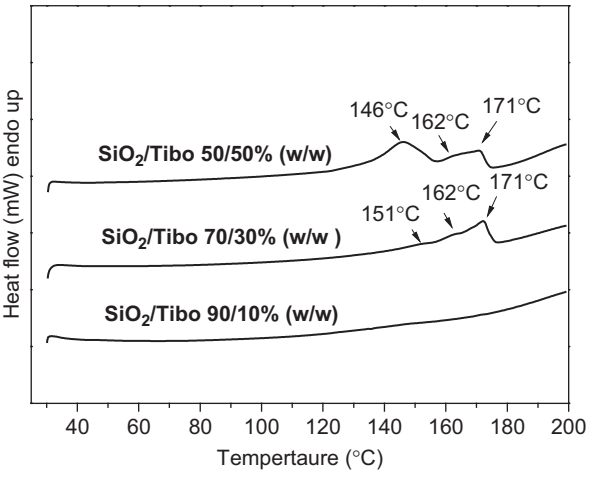

Figure 2. DSC thermograms of SiO_2/Tibo solid dispersion samples prepared by solvent evaporation.

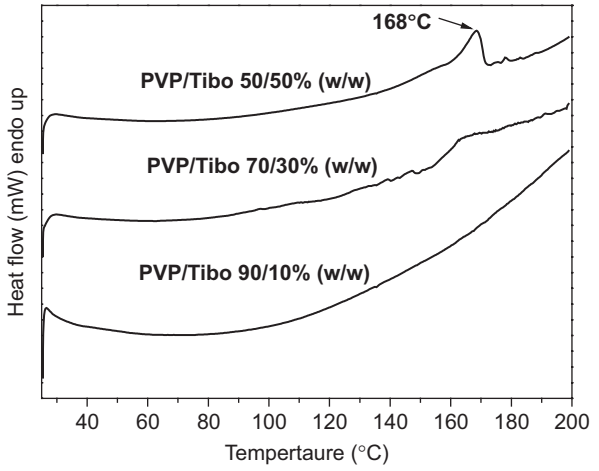

Figure 3. DSC thermograms of PVP/Tibo solid dispersion samples prepared by solvent evaporation.

the samples of SiO_2/Tibo 70/30 and 50/50% (w/w), the DSC thermograms demonstrate that the drug appears crystalline (Figure 2). The peaks in both cases appear to be broader than the pure drug and having a lower intensity, giving a strong impression that a small amount of Tibo is possibly in the amorphous state. Also, at these samples several additional peaks, apart from the main peak, are detected. The sample with 30% (w/w) Tibo exhibits three different peaks at 151°C, 162°C, and 171°C. The first and the second present very low intensities, which is a characteristic feature when the drug is recrystallized in an SD. Owing to the carrier effect, the formed crystals may have different degrees of perfection that leads to melting points at lower temperatures than the initial one[25]. For the sample containing 50% (w/w) Tibo, the first peak recorded at 146°C has higher intensity than the peak attributed to the crystal form of the initial drug at 171°C. This first peak appears 25°C lower than the melting point of the pure drug. A third peak at 162°C is also present, but it is uncertain whether there is an extended overlapping with the observed peak of neat Tibo. As previously reported, variations in the melting peak position could be caused by different binding forces between drug molecules and adsorbent[12]. Furthermore, it is possible for the drug to crystallize in different crystal forms, which may have different melting temperatures contrary to Tibo.

For the binary SD systems of Tibo with PVP, the melting peak of the drug is only observed in the case of the sample containing 50% (w/w) Tibo (Figure 3). Also, in this case, the characteristic melting peak appears to be broader than that of the pure drug and has a lower intensity. Nevertheless it remains close to the melting peak of pure Tibo, only 3°C lower. For the other samples, only a glass transition temperature is detected, which is positioned at lower temperatures than that of the corresponding PVP and at higher temperatures than that of Tibo. Single T_g indicates that probably Tibo is molecularly dispersed into the polymer matrix[26]. Similar are the observations of the DSC thermograms when ternary systems PVP/SiO_2/Tibo were studied. Only the melting points of samples containing higher than 50% (w/w) Tibo were recorded (data not shown).

Wide-angle X-ray diffractometry

WAXD was also used as a complementary method in order to study the physical and crystal state of the drug[27,28]. WAXD pattern of pure Tibo showed that the drug is in a crystalline state, with characteristic diffraction peaks at 2θ = 14.15°, 15.3°, 16.31°, 17.71°, 18.65°, 20.73°, 21°, 23.74°, 24.32°, 27.67°, 23.6°, and 35.37°, which correspond to the crystalline pure form known as Form II (Figure 4a). Also, the WAXD pattern of recrystallized Tibo from ethanol was obtained in order to identify whether the solvent treatment used for the preparation of SDs had any effect on the crystalline form. As can be seen in Figure 4a, the patterns of recrystallized Tibo are completely different from that on neat Tibo. Characteristic peaks are recorded at 2θ = 13.74°, 15.26°, 16.1°, 17.45°, 17.81°, 18.4°, 19.34°, 20.32°, 21.23°, 21.67°, 23.88°, 28.07°, 33.56°, and 37.37°, indicating that Tibo was crystallized in a different form than the previous one, this one referred to as Form I[29].

Results obtained from X-ray diffraction (XRD) patterns indicate that when SiO_2 is used as drug carrier, Tibo appears in an amorphous form for the sample of SiO_2/Tibo 90/10% (w/w) (Figure 4b), as was already found by DSC. It seems that the large specific area of SiO_2 is the main reason for the amorphization of the drug. As the weight ratio of Tibo increases (30% and 50%, w/w) it seems that the carrier cannot keep the drug in an amorphous state, since an oversaturated SD is produced and the characteristic peaks of crystalline Tibo of Form I also appear in the WAXD pattern. Furthermore, some peaks of lower magnitude of crystal Form II are also recorded. This different crystalline form of Tibo can also explain the multiple peaks of melting points observed in the DSC thermograms of the particular samples. When PVP is used as drug carrier, Tibo remains amorphous until the ratio of 30% (w/w) and, only for the sample of PVP/Tibo 50/50% (w/w), the drug crystallizes containing both Forms I and II. Comparing the two carriers it can be stated that PVP is more effective than SiO_2, since it prohibits drug recrystallization at higher drug loading than SiO_2. This may be ascribed to the stronger interactions that may take place between PVP and Tibo than between SiO_2 and Tibo. Silica nanoparticles are inorganic materials and thus the interactions with Tibo may be limited. Consequently, the formation of SDs where the drug is amorphous can be

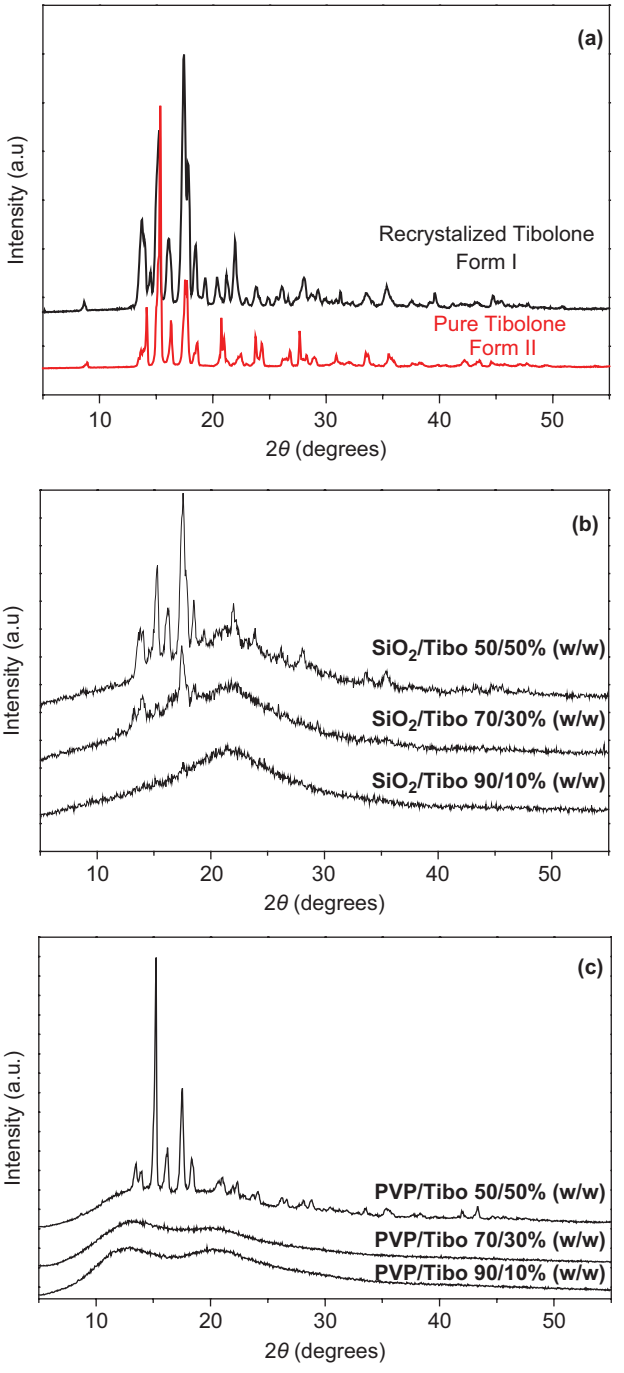

Figure 4. WAXD patterns of (a) pure and recrystallized Tibo from ethanol, (b) SiO_2/Tibo formulations, and (c) PVP/Tibo solid dispersions prepared by solvent evaporation.

attributed only to the finer dispersion of the drug on the large specific surface of SiO_2 and not to possible interactions that may take place between the drug and carrier.

In the case of the ternary PVP/SiO_2/Tibo SDs, the only sample that gives the characteristic peaks of the drug is the one that contains Tibo in 50 % (w/w) (Figure 5). This is in agreement with the DSC results. The combination of

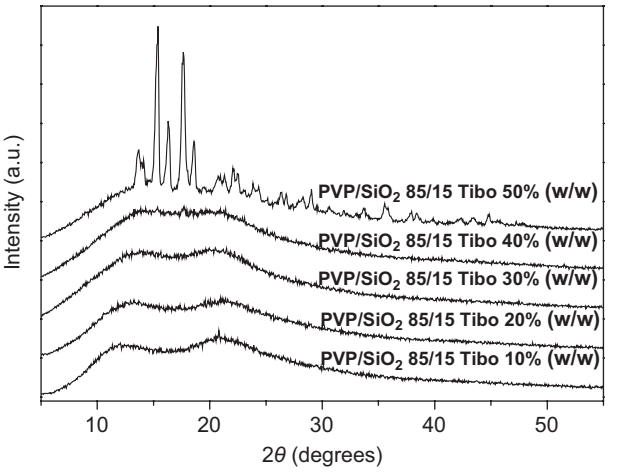

Figure 5. WAXD patterns of PVP/SiO_2/Tibo ternary solid dispersion systems.

the two carriers (PVP and SiO_2) seems to create a new carrier that drastically prevents drug crystallization at higher drug loading. Some interactions with the drug may also be responsible for this behavior.

Fourier transform infrared spectroscopy

For the investigation of the possible interactions between the drug carriers and Tibo, FTIR spectroscopy was used. Any kind of physicochemical interactions that may take place, like the formation of hydrogen bonds between the carriers and drug, will automatically lead to frequency shifts or splitting in absorption peaks. It has also been previously reported that the intermolecular interactions between drug molecules and silanol groups of silica can be detected with FTIR[30–32]. The FTIR spectra of SiO_2, pure Tibo, Tibo recrystallized from ethanol, and SiO_2/Tibo SDs are shown in Figure 6. The characteristic peaks of the silanol group appear at 3434 cm^{-1} for the surface hydroxyl groups of SiO_2 and at 1101 cm^{-1} for the Si—O bond. Tibo spectra also show some characteristic peaks. At 1714 cm^{-1} the stretching of carbonyl group of Tibo appears. The —OH stretching frequencies give a single absorption band at 3492 cm^{-1} in the case of crystallized Tibo in initial crystal Form II and a double absorption band at 3492 and 3410 cm^{-1} in the case of recrystallized Tibo (crystal Form I). The latter double peak appears in the spectra of SiO_2/Tibo 50/50 and also at 70/30% (w/w) dispersions, indicating that Tibo also crystallizes in Form I in these SDs. This appears to be in agreement with the XRD findings, which indicated that Tibo is also crystallized in a different form compared to the initial material.

Examining more carefully the spectra of SDs of binary systems, SiO_2/Tibo, it can be seen that there are no significant shifts in the absorbance of the hydroxyl groups of Tibo and Si—O groups of SiO_2 in the SD

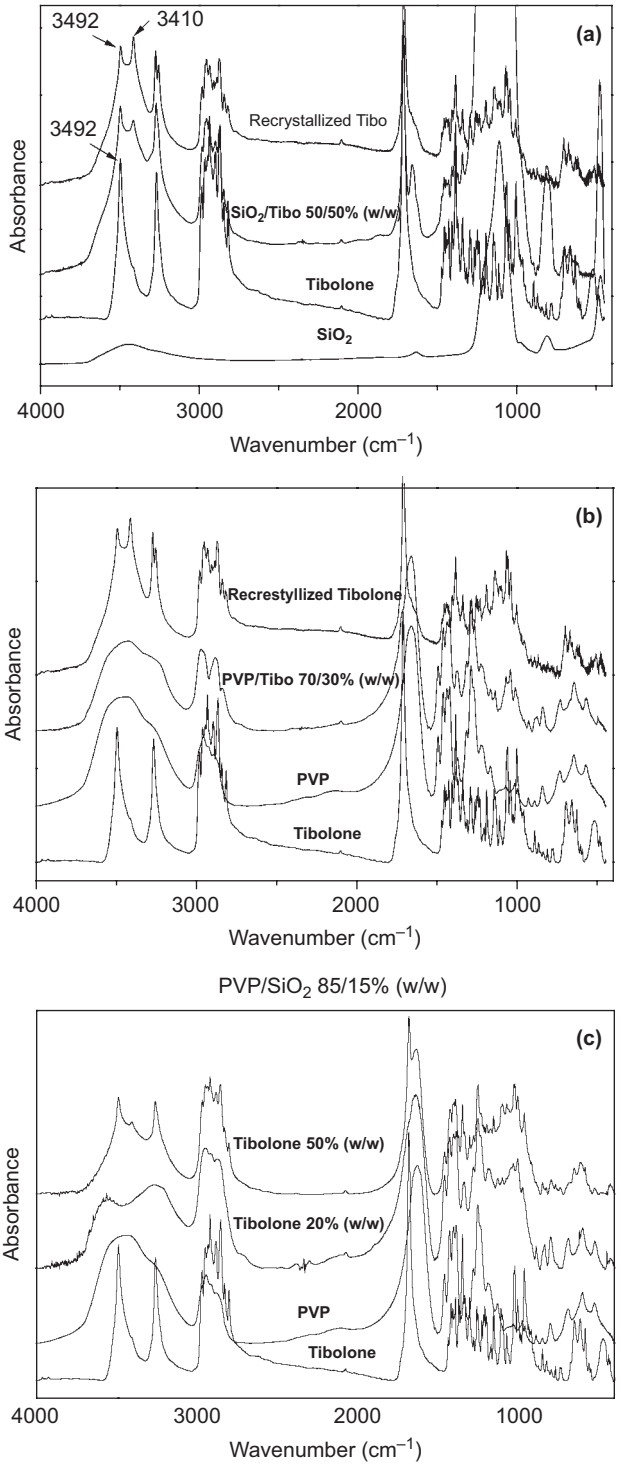

Figure 6. FTIR spectra of (a) SiO_2/Tibo, (b) PVP/Tibo, and (c) ternary solid dispersion of PVP/SiO_2/Tibo in different proportions of Tibo 20 and 50% (w/w).

samples compared to the pure constituents of the dispersions (differences of 1–2 cm^{-1} can be observed, which are close to the experimental error). Thus, it is not possible to establish the existence of interactions between Tibo and SiO_2 matrix based on the absorbances of these groups. However, there are significant differences in the absorbance of the carbonyl group of Tibo. Except for the main peak, which is recorded close to 1714 cm^{-1}, a second peak is recorded at 1658 cm^{-1}. This shift to lower intensity is an indication that hydrogen bonding interactions have developed between the >C=O group of Tibo and the surface hydroxyl groups of SiO_2. Also the intensity of the two characteristic peaks of recrystallized Tibo at 3492 and 3410 cm^{-1}, as it appears in the sample of SiO_2/Tibo 50/50% (w/w), is different. In particular, the intensity of the peak at 3410 cm^{-1} is lower, indicating that although the drug is in crystal form, as it was justified from XRD patterns, it mainly appears with the polymorphous Form II, which is in agreement with the findings of XRD.

In PVP, the absorption band due to stretching of the carbonyl group appears at the frequency region around 1660 cm^{-1}, while the peak at 1291 cm^{-1} is attributed to the N—C group (Figure 6b). These two groups can potentially form hydrogen bond with the drug at molecular level in SD formulations. However, the steric hindrance in the case of N—C precludes the involvement of the nitrogen atom in the creation of intramolecular interactions with the form of hydrogen bonds[11]. The significant broadness of the two characteristic peaks of Tibo at 3492 and 3262 cm^{-1}, and the shift of the peak that appears at 3492 cm^{-1}, at a lower wavelength, indicates the presence of hydrogen bond interactions between free hydroxyl group of Tibo and carbonyl group of PVP. These interactions are probably the reason for drug amorphization.

From the FTIR spectra of the ternary SD systems, the significant broadness of the hydroxyl groups of Tibo appears, with a more defined way and, at the same time, the peak of the carbonyl group of PVP is characteristically broadened (Figure 6c). This fact justifies the existence of a hydrogen bond between the carbonyl group of Tibo and the carbonyl groups of PVP. Also, some weak interaction between the hydroxyl groups located on the surface of silica and the carbonyl group of the drug are possible.

Scanning electron microscopy

Using the SEM it is possible to have a more detailed look on the morphology of the prepared SDs. As can be seen in Figure 7, in PVP SD containing 50% (w/w) Tibo, well-formed crystals appear on the surface of the polymer matrix. This is in agreement with DSC and XRD data from which it was found that the drug crystallizes at such concentrations. In the case where SiO_2 was used as drug carrier, the drug is dispersed on the nanoparticles surface (Figure 8). At concentrations up to 20% (w/w) Tibo, since the drug is amorphous, no crystals are detected. However, even at higher concentrations, where the drug is in

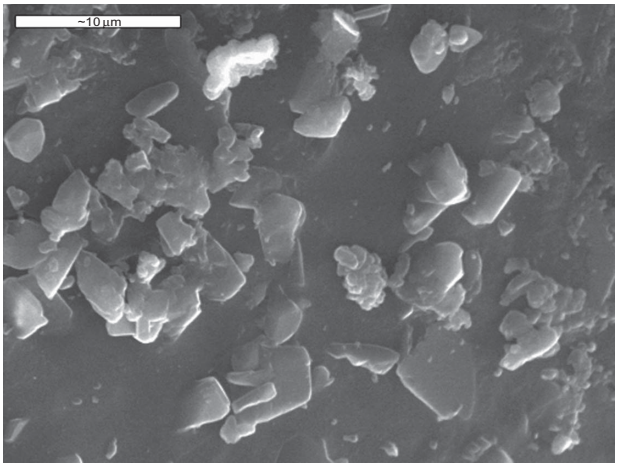

Figure 7. SEM micrographs of PVP/Tibo solid dispersions containing (a) 40% (w/w) and (b) 50% (w/w) Tibo.

crystalline form, these crystals are hardly detectable. It seems that due to the large available surface Tibo may form nanocrystals on the nanoparticles' surface.

Release profile

The in vitro release profile of Tibo for the binary SD systems of PVP/Tibo and SiO_2/Tibo are shown in Figure 9. It seems that in the case of PVP (Figure 9a), the ability of the polymer matrix to create amorphous SDs constitutes the main reason for the immediate release of the drug. For the samples containing 10% and 30% (w/w) Tibo, the drug release is almost completed in 30 minutes. However, as the drug content increases, the release rate of the drug is characteristically decreased.

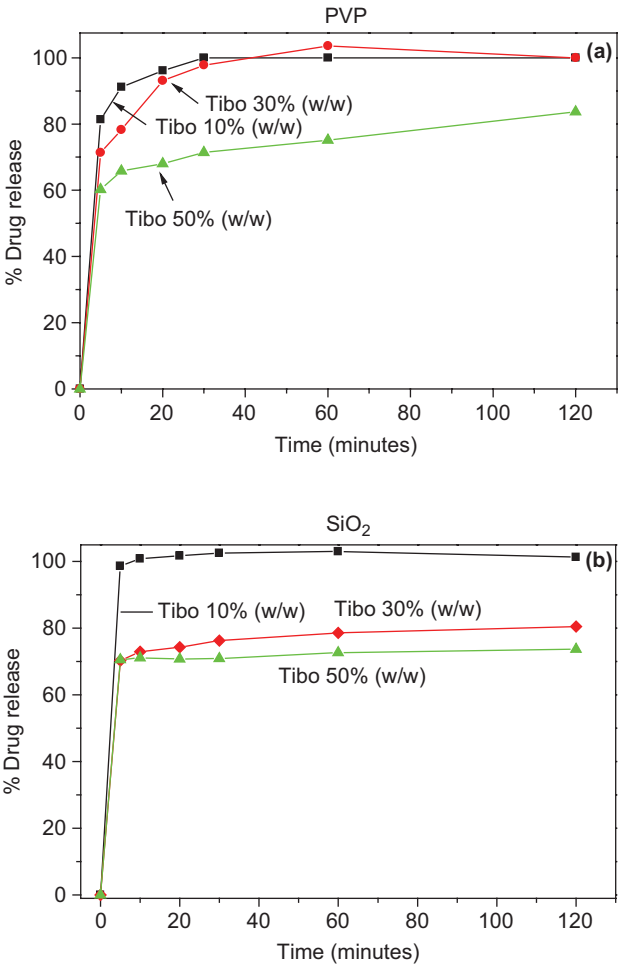

Figure 9. The release profiles of Tibo solid dispersions with (a) PVP and (b) SiO_2 as matrix carriers.

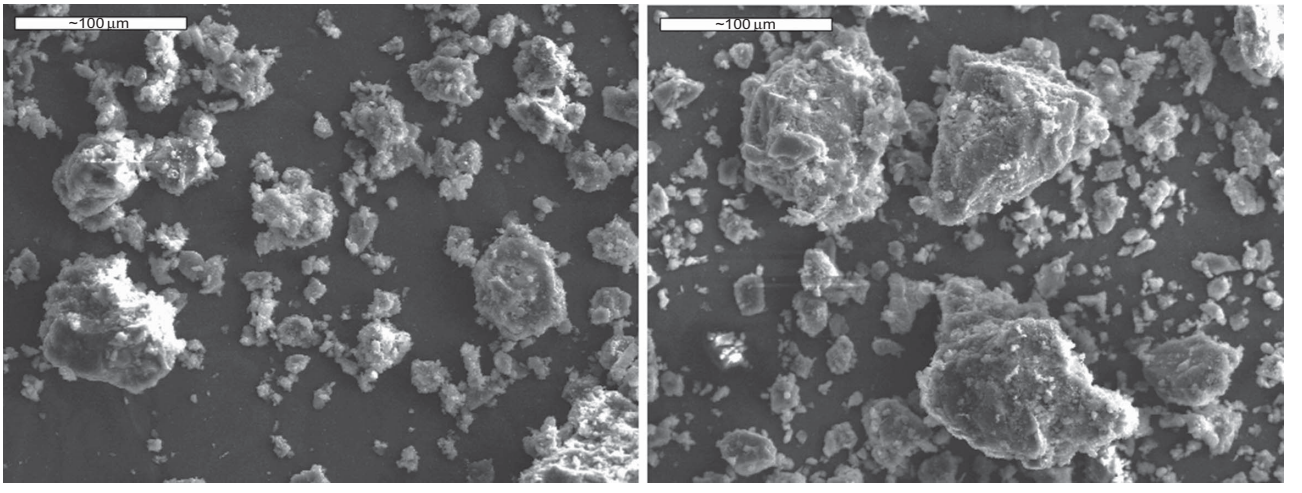

Figure 8. SEM micrographs of SiO_2/Tibo solid dispersions containing (a) 20% (w/w) and (b) 50% (w/w) Tibo.

The lower dissolution rate is attributed to the crystallization of the drug at the particular SD.

In the case of SiO_2/Tibo binary systems, the immediate release for the samples containing 10% (w/w) Tibo is attributed to the large specific area of silica that enables the fine distribution of the drug onto the nanoparticles surface[12], and the eventual amorphization of the drug. Furthermore, this result implies that the hydrophilic properties of the silica particles contributed to the improvement of wettability and, finally, improvement of the drug dissolution from SD, as reported previously[30]. For the samples containing 30 and 50 wt% Tibo, the drug release also seems to be fast initially, reaching 70–80% in 20 minutes, but eventually, even after 2 hours, the release of the drug is not fully completed. It seems that the silica nanoparticles can form some kind of strong interactions with the drug, as was verified from the FTIR spectra, and thus it cannot be completely released. Additionally, the release rate of these samples is lower due to the crystallization of the drug.

Comparing the release rate of two different matrices it can be stated that there are no obvious differences for the dispersions containing 10 wt% Tibo. In both matrices the drug is amorphous and dissolves immediately. Also, in the other two concentrations, it seems that the physical state of the drug (crystalline or amorphous), and the extent of interactions control the release rate and not the drug carrier.

In ternary PVP/SiO_2/Tibo SD systems, the release profiles seem to differ. From Figure 10 it can be seen that the release rate decreases as the drug content increases. Also, it is remarkable that for the samples with 10 and 20 wt% of Tibo, the release rate of the drug seems to be faster in comparison to the binary SD systems with PVP, a fact that probably is the result of the combined action of PVP and silica nanoparticles. However, the most impressive result is the release profile of the samples with higher than 40 wt% content in Tibo. The release of Tibo is completed in 5 hours, accomplishing a release that can be characterized as sustained rather than immediate. This is more pronounced in the sample containing 50% (w/w) of Tibo. Since such a release profile was not observed when the two matrices were used separately (PVP/Tibo or SiO_2/Tibo), it can be considered that during solvent mixing of the two materials (PVP/SiO_2) and after solvent evaporation a new matrix has formed. The physicochemical characteristics of this PVP/SiO_2 nanocomposite matrix may be different compared to the initial materials. Examining the literature it was found that PVP interacts with the silanol groups of SiO_2[33]. As reported, the PVP molecules are not washed by the silica surfaces when the ratio $C_{PVP}/C_{SiO_2} \leq 0.1$ because of bonding in multicentered adsorption complexes, creating a monolayer of PVP on the nanoparticles' surface. The energy of these hydrogen bonds as calculated according to Kitaura–Morokuma method is $\Delta E_{HF} = -41$ kJ/mol[34]. To verify that the characteristics of PVP/SiO_2 are different than the initial materials, PVP/SiO_2 nanocomposites containing different silica content were prepared with solvent evaporation method and studied.

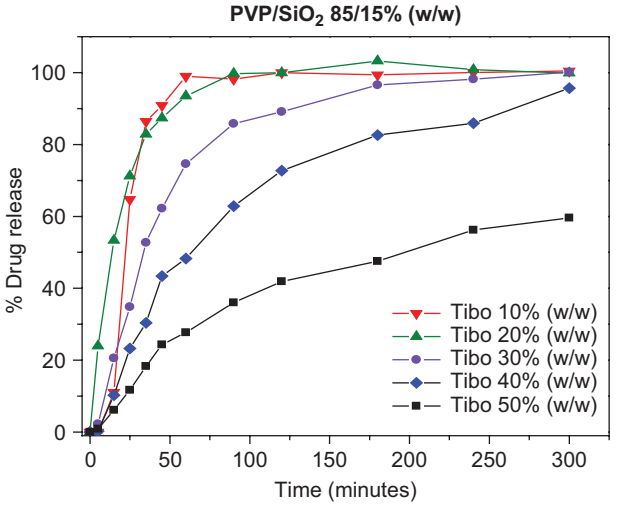

Figure 10. The release profiles of Tibo solid dispersions with ternary solid dispersion of PVP/SiO_2/Tibo with different drug content.

Characterization of PVP/SiO_2 nanocomposites

After solvent evaporation it is observed that the PVP/SiO_2 nanocomposites are transparent, which is an indication that nanoparticles are finely dispersed in the polymer matrix. From DMA studies it was revealed that as the amount of silica nanoparticles increased the material became stiffer. Storage modulus in all nanocomposites at low as well as at high temperatures is much higher than the storage modulus of pure PVP. The glass transition temperature (T_g) is often obtained by either the temperature at which the dynamic loss modulus is at a peak height or the temperature at which the loss tangent tanδ (E''/E') exhibits a peak. As can be seen from tanδ variation (Figure 11) there is a shift of only 1–2°C of T_g in higher temperatures. Such an increase in the glass transition temperature of polymer nanocomposites is very common due to the formed interphase between nanoparticles and polymer matrix. Macromolecules placed at this interphase have lower mobility, especially when interactions develop between the components, resulting in an increase in the rigidity of the nanocomposites. However, this increase is very small, indicating that the evolved interactions are weak rather than strong.

In order to evaluate the effect of hydrogen bonding between PVP and SiO_2 their spectra were collected. Fumed silica bears three kinds of surface hydroxyl groups: (i) isolated free (single silanols), ≡SiOH; (ii) geminal free (geminal silanols or silanediols), $=Si(OH)_2$; and (iii) vicinal,

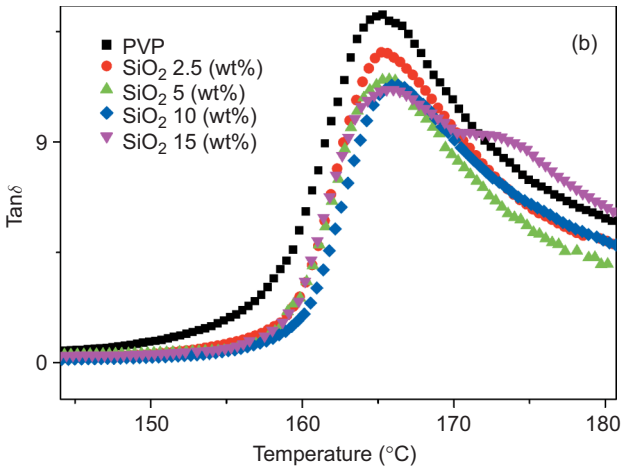

Figure 11. Dynamic mechanical scans of PVP/SiO_2 nanocomposites as function of temperature. Variation of tanδ.

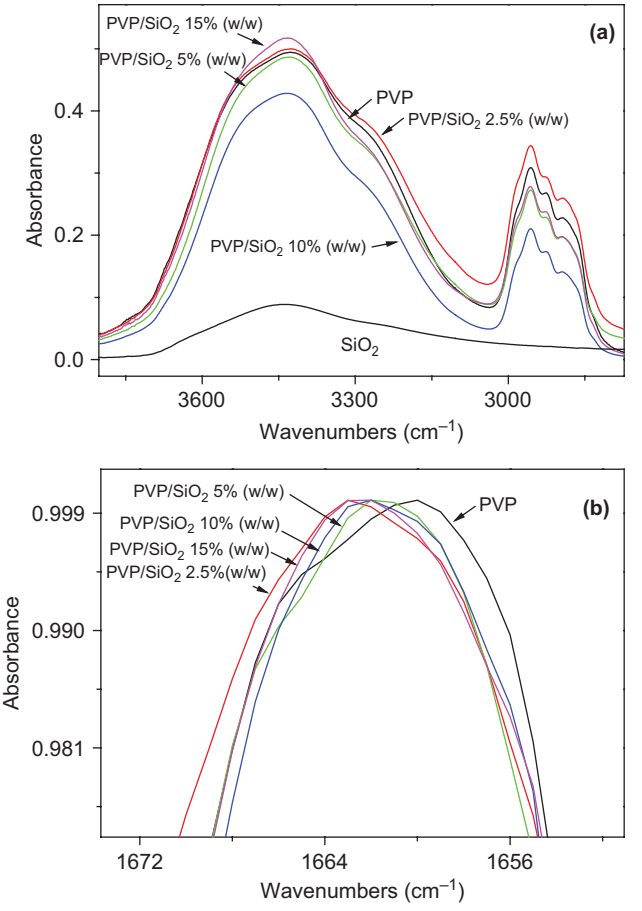

Figure 12. FTIR spectra of PVP/SiO_2 nanocomposites.

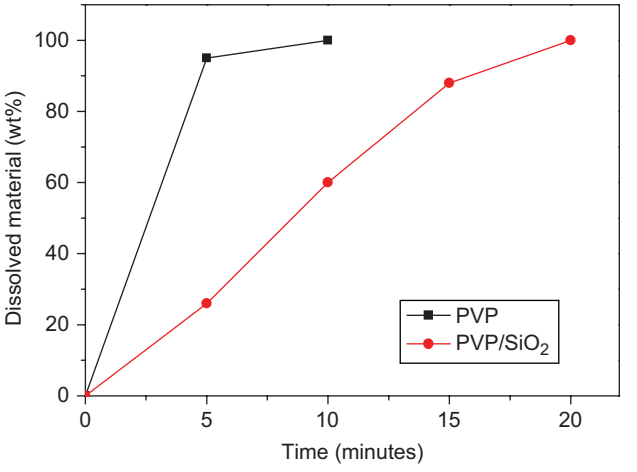

Figure 13. PVP and PVP/SiO_2 dissolution rates in water.

OH groups bound together through hydrogen bond (H-bonded single silanols, H-bonded geminals, and their H-bonded combinations). The —OH stretching vibration of hydrogen-bonded silanol groups can be observed at 3438 cm^{-1}, while the peak corresponding to the free hydroxyl groups at 3747 cm^{-1} is very weak and hardly detectable (Figure 12). However, the most intense peak of SiO_2 is that corresponding to Si—O—Si groups recorded in the FTIR spectrum at 1111 cm^{-1}. From the FTIR spectra of the prepared nanocomposites it is obvious that the characteristic peaks of Si—O—Si remained unaffected and are recorded at the same wavenumber as in pure SiO_2, while from the Si—O absorbance at 3438 cm^{-1} there is only a small shift to 3432 cm^{-1}. However, at this position PVP also exhibits a strong peak and thus it is not possible to evaluate the possible interactions that take place. Examining the wavenumber of the carbonyl groups of PVP a small shift can be seen at slightly higher positions, from 1660 to 1662 cm^{-1} (Figure 12b). This shift is evidence that the carbonyl groups of PVP participated in hydrogen bonds with the reactive groups of SiO_2. However, since the difference between the absorbance in neat PVP and its nanocomposites is very small, it must be concluded that these interactions are of low intensity. This is in accordance with the DMA results, where only a small shift was observed on the nanocomposites' T_g.

The aforementioned interactions and the incorporation of SiO_2 nanoparticles into PVP matrix have changed the physicochemical characteristics of the PVP carrier as well as the solubility of PVP in water. For this reason 1 g of PVP and PVP/SiO_2 in the form of films were added to the dissolution medium. The films were removed every 5 minutes and weighted to measure the dissolved material. As can be seen in Figure 13 neat PVP dissolves almost immediately in water in less than 10 minutes. After SiO_2 addition the matrix became more hydrophobic and the dissolution rate was reduced. Silica nanoparticles are inorganic materials, which cannot be dissolved in water but can form a gel. This gel and the ability of carbonyl groups of PVP to

interact with the silanol groups of SiO_2 result in fewer reactive groups of PVP available for interaction with the water molecules (Figure 13). Thus, the dissolution rate of PVP became lower and the PVP/SiO_2 matrix dissolves completely only after 20 minutes. This is the main reason why the release profiles of Tibo from ternary SD of PVP/SiO_2/Tibo are different compared to neat PVP or SiO_2.

Conclusions

Dissolution rate of poorly water-soluble drug Tibo was drastically enhanced by the preparation of SDs with PVP and silica nanoparticles. At low drug loadings (up 30% (w/w) amorphization of the drug was achieved for both matrices, while at higher concentrations the drug was in crystalline form. However, even in that case, the particle size of the drug was reduced compared to the neat drug. Interactions that took place between hydroxyl groups of Tibo and reactive groups of PVP or SiO_2 nanoparticles were responsible for this behavior. When the concentration of Tibo in SD samples was low, the drug was released almost immediately from PVP/Tibo and SiO_2/Tibo SDs, whereas at higher concentrations the release became slower. The drug dissolution rate was changed when ternary SDs of PVP/SiO_2/Tibo were prepared, especially for drug concentrations higher than 30% (w/w). When the concentration of Tibo increased, the release rate tended to decrease, giving an almost sustained release of the drug. This was because the physicochemical characteristics of the PVP matrix were altered after the incorporation of the silica nanoparticles.

Acknowledgments

This work was funded by the Greek Ministry of Development under the 3rd European Community Support Framework, Operational Program 'Competiveness' 2000–2006 (PENED, 78108).

Declaration of interest: The authors report no conflicts of interest.

References

1. Serajuddin TM. (1999). Solid dispersion of poorly water-soluble drugs: Early promises, subsequent problems, and recent breakthroughs. J Pharm Sci, 88:1058–66.
2. Miller DA, DiNunzio JC, Yang W, James McGinity W, Williams III RO. (2008). Targeted intestinal delivery of supersaturated itraconazole for improved oral absorption. Pharm Res, 25:1450–9.
3. Overhoff KA, Moreno A, Miller DA, Johnston KP, Williams III RO. (2007). Solid dispersions of itraconazole and enteric polymers made by ultra-rapid freezing. Int J Pharm, 336:122–32.
4. Karavas E, Georgarakis E, Sigalas MP, Avgoustakis K, Bikiaris D. (2007a). Investigation of the release mechanism of a sparingly water-soluble drug from solid dispersions in hydrophilic carriers based on physical state of drug, particle size distribution and drug–polymer interactions. Eur J Pharm Biopharm, 66:334–47.
5. Papageorgiou GZ, Bikiaris D, Kanaze FI, Karavas E, Stergiou A, Georgarakis E. (2008). Tailoring the release rates of fluconazole using solid dispersions in polymer blends. Drug Dev Ind Pharm, 34:336–46.
6. Leuner C, Dressman J. (2000). Improving drug solubility for oral delivery using solid dispersions. Eur J Pharm Biopharm, 50:47–60.
7. Karavas E, Georgarakis M, Docoslis A, Bikiaris D. (2007b). Combining SEM, TEM, and micro-Raman techniques to differentiate between the amorphous molecular level dispersions and nanodispersions of a poorly water-soluble drug within a polymer matrix. Int J Pharm, 340:76–83.
8. Papageorgiou GZ, Bikiaris D, Karavas E, Docoslis A, Stergiou A, Georgarakis E. (2006). Effect of physical state and particle size distribution on dissolution enhancement of nimodipine/PEG solid dispersions prepared by melt mixing and solvent evaporation. AAPS J, 8(4):E623–31.
9. Miller DA, McConville JT, Yang W, Williams III RO, McGinity JW. (2007). Hot-melt extrusion for enhanced delivery of drug particles. J Pharm Sci, 96:361–76.
10. Chiou WL, Riegelman S. (1971). Pharmaceutical applications of solid dispersion system. J Pharm Sci, 60:1281–302.
11. Taylor LS, Zografi G. (1997). Spectroscopic characterization of interactions between PVP and indomethacin in amorphous molecular dispersion. Pharm Res, 14:1691–8.
12. Friedrich H, Fussnegger B, Kolter K, Bodmeier R. (2006). Dissolution rate improvement of poorly water-soluble drugs obtained by adsorbing solutions of drugs in hydrophilic solvents onto high surface area carriers. Eur J Pharm Biopharm, 62:171–7.
13. Takeuchi H, Nagira S, Yamamoto H, Kawashima Y. (2004). Solid dispersion particles of tolbutamide prepared with fine silica particles by the spray-drying method. Pow Tech, 141:187–95.
14. Watanabe T, Ono I, Wakiyama N, Kusai A, Senna M. (2002). Controlled dissolution properties of indomethacin by compounding with silica. STP Pharm Sci, 12:363–7.
15. Pokharkar VB, Mandpe LP, Padamwar MN, Ambike AA, Mahadik KR, Paradkar A. (2006). Development, characterization and stabilization of amorphous form of low T_g drug. Pow Tech, 167:20–5.
16. Ambike AA, Mahadik KR, Paradkar A. (2005). Spray-dried amorphous solid dispersions of simvastatin, a low T_g drug: *In vitro in vivo* evaluations. Pharm Res, 22:990–8.
17. Sator K, Sator MO, Sator PG, Egarter C, Huber JC. (2006). Effects of tibolone on selectins in postmenopausal women. Maturitas, 53:166–70.
18. Kloosterboer HJ. (2004). Tissue-selective effects of tibolone on the breast. Maturitas, 49:S5–15.
19. Reeda MJ, Kloosterboer HJ. (2004). Tibolone: A selective tissue estrogenic activity. Maturitas, 48:S4–6.
20. Schatz F, Kuczynski E, Kloosterboer HJ, Buchwalder L, Tang C, Krikun G, et al. (2005). Tibolone and its metabolites enhance tissue factor and PAI-1 expression in human endometrial stroma l-cells. Evidence of progestogenic effects. Steroids, 70:840–5.
21. Kloosterboer HJ. (2001). Tibolone: A steroid with a tissue-specific mode of action. J Ster Biochem Mol Biol, 76:231–8.
22. Kloosterboer HJ. (2004). Tissue-selectivity: The mechanism of action of tibolone. Maturitas, 48(1):S30–40.
23. De Haan P. (2004). Immediate-release pharmaceutical dosage form comprising polymorphous Tibolone. N.V. Organon 5340 BH Oss (NL), Proprietor: Akzo Nobel N.V. 6824 BM Arnhem (NL), EP 1 499 278 B1.

24. Papadimitriou SA, Bikiaris D, Avgoustakis K. (2008). Microwave-induced enhancement of the dissolution rate of poorly water-soluble Tibolone from poly(ethylene glycol) solid dispersions. J Appl Polym Sci, 108:1249–58.
25. Kanaze FI, Kokkalou E, Niopas I, Georgarakis M, Stergiou A, Bikiaris D. (2006). Thermal analysis study of flavonoid solid dispersions having enhanced solubility. J Therm Anal Cal, 83:283–90.
26. Gupta P, Thilagavathi R, Chakraborti AK, Bansal AK. (2005). Role of molecular interactions in stability of celecoxib-PVP amorphous systems. Mol Pharm, 2:384–91.
27. Bikiaris D, Papageorgiou GZ, Stergiou A, Pavlidou E, Karavas E, Kanaze F, et al. (2005). Physicochemical studies on solid dispersions of poorly-water soluble drugs. Evaluation of capabilities and limitations of thermal analysis techniques. Thermochim Acta, 439:58–67.
28. Hu J, Rogers TL, Brown J, Young T, Johnston KP, Williams III RO. (2002). Improvement of dissolution rates of poorly water soluble APIs using novel spray freezing into liquid technology. Pharm Res, 19:1278–84.
29. Sas GAJMT, van Doornum EM. (1991). Pharmaceutical composition which contains a pharmaceutically suitable carrier and the compound having the structure (7a,17a)-17-hydroxy-7-methyl-19-nor-17-pregn-5(10)-en-20-yn-3-one. US Patent 5,037,817.
30. Wang L, Cui FD, Sunada H. (2006). Preparation and evaluation of solid dispersions of Nitredipine prepared with fine silica particles using the melt-mixing method. Chem Pharm Bull, 54:37–43.
31. Takeuchi H, Nagira S, Yamamoto H, Kawashima Y. (2005). Solid dispersion particles of amorphous indomethacin with fine porous silica particles by spray-drying method. Int J Pharm, 293:155–64.
32. Takeuchi H, Handa T, Kawashima Y. (1987). Spherical solid dispersion containing amorphous tolbutamide embedded in enteric coating polymers or colloidal silica prepared by spray-drying technique. Chem Pharm Bull, 5:3800–6.
33. Hsiao CN, Huang KS. (2005). Synthesis, characterization, and applications of polyvinylpyrrolidone/SiO_2 hybrid materials. J Appl Polym Sci, 96:1936–42.
34. Gun'ko VM, Voronin EF, Nosach LV, Pakhlov EM, Voronina OE, Guzenko NV, et al. (2006). Nanocomposites with fumed silica/poly(vinyl pyrrolidone) prepared at a low content of solvents. Appl Surf Sci, 253(5): 2801–11.